18. Supplemental Web movie is available at www.sciencemag.org/feature/data/1053788.shl
19. P. M. Fishbane, S. Gasiorowicz, S. T. Thornton, *Physics for Scientists and Engineers* (Prentice-Hall, Upper Saddle River, NJ, ed. 2, 1996), p. 419.
20. H. J. Leisi, *Klassische Physik* (Birkhäuser Verlag, Basel, Switzerland, 1996), pp. 274–276.
21. Nonuniform fields produce different precessional periods. See J. E. Mercereau and R. P. Feynman [*Phys. Rev.* **104**, 63 (1956)].
22. By "center," we mean a region with linear size comparable to the spatial resolution of our experiment.
23. This nonuniformity cannot affect the precessional period because the initial field pulse is one of the "small" quantities that can be neglected in solving the Larmor equation.
24. We use $\delta \approx 200$ nm, from J. D. Jackson [*Classical Electrodynamics* (Wiley, New York, 1962), p. 225, equation 7.85]. On this time scale, the magnetic permeability is taken to be 1 because the magnetization is not yet aligned along the magnetic field direction (H. C. Siegmann and W. Hunziker, personal communication).
25. After this initial delay, eddy currents are negligible for two reasons: the oscillation of the magnetization occurs on a larger time scale and eddy currents do not affect the precessional motion in the present geometry (*3*).
26. M. R. Freeman, J. F. Smyth, *J. Appl. Phys.* **79**, 5898 (1996).
27. A. Y. Elezzabi, M. R. Freeman, *Appl. Phys. Lett.* **68**, 3546 (1996).
28. We gratefully acknowledge financial support by the Swiss National Fund and the Swiss Federal Institute of Technology.

7 July 2000; accepted 8 September 2000

Modulation Instability and Pattern Formation in Spatially Incoherent Light Beams

Detlef Kip,[1,2] Marin Soljacic,[1,3] Mordechai Segev,[1,4]* Eugenia Eugenieva,[5] Demetrios N. Christodoulides[5]

We report on the experimental observation of modulation instability of partially spatially incoherent light beams in noninstantaneous nonlinear media and show that in such systems patterns can form spontaneously from noise. Incoherent modulation instability occurs above a specific threshold that depends on the coherence properties (correlation distance) of the wave packet and leads to a periodic train of one-dimensional filaments. At a higher value of nonlinearity, the incoherent one-dimensional filaments display a two-dimensional instability and break up into self-ordered arrays of light spots. This discovery of incoherent pattern formation reflects on many other nonlinear systems beyond optics. It implies that patterns can form spontaneously (from noise) in diverse nonlinear many-body systems involving weakly correlated particles, such as atomic gases at (or near) Bose-Einstein condensation temperatures and electrons in semiconductors at the vicinity of the quantum Hall regime.

Modulation Instability (MI) is a process that appears in most nonlinear wave systems. Because of MI, small amplitude and phase perturbations (from noise) grow rapidly under the combined effects of nonlinearity and diffraction (or dispersion, in the temporal domain). As a result, a broad optical beam [or a quasi–continuous wave (quasi-CW) pulse] tends to disintegrate during propagation (*1–4*), leading to filamentation (*5*, *6*) or to break up into pulse trains (*1–4*). MI typically occurs in the same parameter region where another universal phenomenon, soliton occurrence, is observed. Solitons are stationary localized wave packets (wave packets that never broaden) that share many features with real particles. For example, their total energy and momentum is conserved even when they interact with one another (*7*). Solitons can be intuitively understood as a result of the balance between the broadening tendency of diffraction (or dispersion) and nonlinear self-focusing. A soliton forms when the localized wave packet induces a potential (via the nonlinearity) and "captures" itself in it, thus becoming a bound state in its own induced potential. In the spatial domain of optics, a spatial soliton forms when a very narrow optical beam induces (through self-focusing) a waveguide structure and guides itself in its own induced waveguide. The relation between MI and solitons is best manifested in the fact that the filaments (or the pulse trains) that emerge from the MI process are actually trains of almost ideal solitons. Therefore, MI can be considered to be a precursor to soliton formation. To date, MI has been systematically investigated in connection with numerous nonlinear processes. Yet traditionally, it was always believed that MI is inherently a coherent process and can only appear in nonlinear systems with a perfect degree of spatial and temporal coherence. On the other hand, recent theoretical work (*8*) has shown that MI can also exist in relation with partially incoherent wave packets or beams. This in turn leads to several important new features: incoherent MI appears only if the "strength" of the nonlinearity exceeds a well-defined threshold that depends on the degree of spatial correlation (coherence). Moreover, by appropriately suppressing MI, new families of solitons are possible that have no counterpart whatsoever in the coherent regime (*9*). Here, we present the experimental observation of modulation instability and pattern formation in partially spatially incoherent light beams in nonlinear media.

Until a few years ago, solitons were considered to be solely coherent entities. However, experimental observations of solitons made of partially spatially incoherent light (*10*) and of temporally and spatially incoherent ("white") light (*11*) have proven that incoherent solitons do exist, and such observations have opened entirely new directions in the field of solitons. Numerous theoretical and experimental works followed soon thereafter, describing bright (*12–15*) and dark (*16*, *17*) incoherent solitons, their interactions (*18*), and stability properties (*19*). The existence of incoherent solitons proves that self-focusing is possible not only for coherent wave packets but also for wave packets upon which the phase is random. The key to their existence is the noninstantaneous nature of the nonlinearity, which responds only to the beam's time-averaged intensity structure and not to the instantaneous highly speckled and fragmented wavefront. In other words, the response time of the nonlinear medium must be much longer than the average time of phase fluctuations across the beam. Thus, the time-averaged intensity induces, through the nonlinearity, a multimode waveguide structure (a potential well that can bind many states), whose guided modes are populated by the optical field with its instantaneous speckled structure. With this noninstantaneous nature of the nonlinearity in mind, we were motivated to find out whether patterns can form spontaneously on a partially coherent uniform beam through the interplay between nonlinearity and diffraction. As a first step, we have shown theoretically (*8*) that a uniform partially incoherent wave front is unstable in such media, provided that the nonlinearity exceeds a well-defined threshold set by the coherence properties. Above that threshold, MI should occur, and patterns should form.

[1]Physics Department and Solid State Institute, Technion, Haifa 32000, Israel. [2]Physics Department, Universität Osnabrück, 49069 Osnabrück, Germany. [3]Physics Department, Princeton University, Princeton, NJ 08544, USA. [4]Department of Electrical Engineering, Princeton University, Princeton, NJ 08544, USA. [5]Electrical Engineering and Computer Science Department, Lehigh University, Bethlehem, PA 18015, USA.

*To whom correspondence should be addressed. E-mail: msegev@techunix.technion.ac.il

The main predictions of the incoherent MI theory (*8*) are as follows. (i) The existence of a sharp threshold for the nonlinear index change, below which perturbations (noise) on top of a uniform input beam decay and above which a quasi-periodic pattern forms. (ii) The threshold depends on the coherence properties of the input beam: the threshold increases with decreasing correlation distance (decreasing spatial coherence). (iii) Saturation alone, although it keeps the maximum index change and correlation distance fixed, arrests the growth rate of the MI and can decrease it to below the MI threshold. In what follows, we describe our experimental results that confirm all of these predictions and also reveal other unexpected features.

In our incoherent MI experiments, we use a strontium-barium niobate crystal and use its photorefractive screening nonlinearity (*20*–*22*). The dimensions of the sample are a by b by c = 7.0 mm by 6.5 mm by 8.0 mm, where light propagation is along the crystalline a-axis and the external electric bias field is applied along the c-axis. At moderate intensities (1 W/cm^2), the response time of our crystal is $\tau \approx 0.1$ s; thus, for any light beam across which the phase varies much faster than τ, the nonlinear crystal responds only to the time-averaged (over times much larger than τ) intensity structure. In our experimental setup, we split a CW argon ion laser beam (of λ = 514.5-nm wavelength) into two beams using a polarizing beam splitter. Each beam is sent through a rotating diffuser, which introduces a random phase varying much faster than τ, acting as a source of partially spatially incoherent light. Following the rotating diffusers the beams are expanded, collimated and made uniform, and recombined using another polarizing beam splitter. Lastly, both beams are launched into the crystal, in which they co-propagate. When an external (bias) direct current field is applied to the crystal, the extraordinarily polarized beam experiences a large index change and, thus, serves as the "signal beam," whereas the ordinarily polarized beam experiences only a tiny index change and, therefore, serves as a background beam [its only role is to tune the degree of saturation of the nonlinearity (*22*)]. A lens and a polarizer are used to capture the image of the signal beam intensity at the output face of the sample in a charge-coupled device (CCD) camera. We control the degree of coherence of the signal beam by adjusting the diameter of the laser beam incident on the rotating diffuser: the larger the beam diameter, the higher the incoherence and the shorter the correlation distance l_c. The background beam is made highly incoherent, which guarantees that it never forms any patterns. We estimate the correlation distance l_c at the input face of the crystal (when the system is linear, that is, when the applied field is zero) as the average value of the full width at half maximum (FWHM) of the speckle size on the CCD camera when the diffuser is momentarily stopped.

Upon application of a sufficiently large bias field to the crystal, the signal beam experiences MI and forms patterns (Fig. 1). When the input signal beam is uniform, the underlying nonlinearity is of the form

$$\delta n = \Delta n_0 \, [1 + (I_0/I_{sat})] \, [I(r)/(I(r) + I_{sat})] \quad (1)$$

where $I(r)$ is the local intensity as a function of coordinate r, I_{sat} is the intensity of the incident background beam, and I_0 is the intensity of the signal beam at the input face. The term $[1 + (I_0/I_{sat})]$ comes from the fact that the total current flowing through the crystal is almost the same as the photocurrent generated by both beams [in contradistinction with the case of bright screening solitons, where the soliton beam is very narrow compared to the crystal width and therefore does not affect the photocurrent and this factor is equal to unity (*20*)]. In Eq. 1, $\Delta n_0 = 0.5 n_e^3 r_{33}$ (V/L) is the electro-optic refractive index change, n_e is the extraordinary refractive index, r_{33} is the electrooptic tensor element, and (V/L) is the externally applied electric field.

Incoherent MI is observed for a nonlinearity δn exceeding a certain threshold. When an external voltage is applied to the nonlinear crystal with a magnitude large enough to allow for MI, the homogeneous light distribution at the output face of the sample becomes periodically modulated and starts to form one-dimensional (1D) filaments of incoherent light. In our experiments, the preferred direction of the stripes is perpendicular to the c-axis of the crystal. We believe that this is due to the existence of striations in our sample, which act as "initial noise" that is eventually amplified by MI. These are index inhomogeneities in planes perpendicular to the c-axis that originate from melt composition changes during growth of the crystal. Another possible reason for the preferential 1D directionality might have to do with the anisotropy of the photorefractive nonlinearity. However, the final orientation of the stripes is rather random, with the largest observed angle of inclination of the stripes relative to the c-axis being roughly 45°. Typical examples of MI of partially spatially incoherent light are shown in Fig. 1, which displays the intensity of the signal beam at the output plane of the crystal. The correlation distance of the incoherent light is l_c=17.5 μm and the intensity ratio I_0/I_{sat} = 1. Figure 1A shows the output intensity without nonlinearity (V/L = 0). The cases of Fig. 1, B through D, correspond to a value of the nonlinearity just

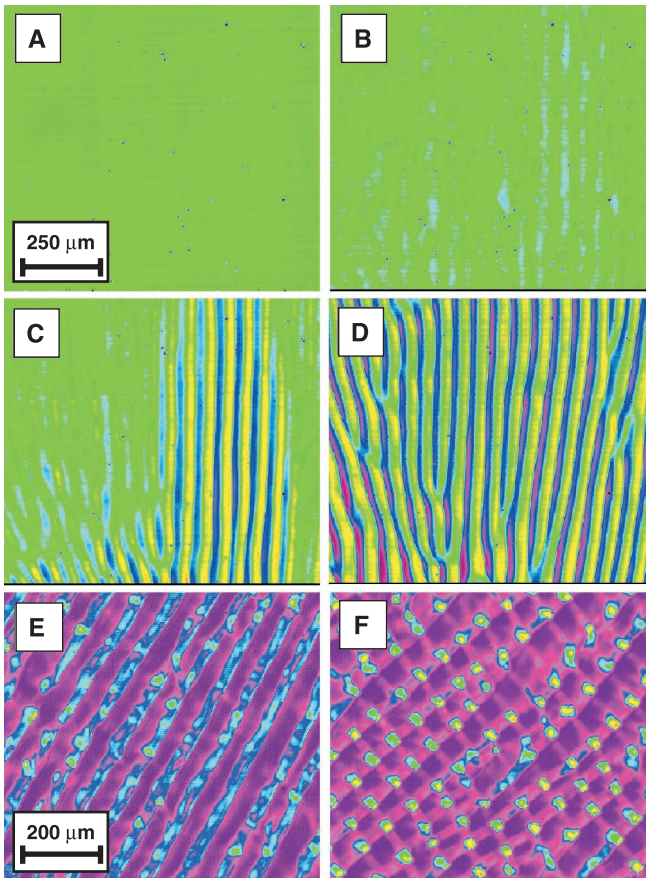

Fig. 1. The intensity structure of a partially spatially incoherent beam at the output plane of the nonlinear crystal. The sample is illuminated homogeneously with partially spatially incoherent light with l_c = 17.5 μm. The displayed area is 1.0 mm by 1.0 mm (**A** through **D**) and 0.8 mm by 0.8 mm (**E** and **F**), respectively. The size of the nonlinear refractive index change of the crystal is successively increased from (A) $\Delta n_0 = 0$ (the linear case), to (B) 3.5×10^{-4}, (C) 4.0×10^{-4}, (D) 4.5×10^{-4}, (E) 9×10^{-4}, and (F) 1×10^{-3}. The plots (B through D) show the cases just below threshold (no features), at threshold (partial features), and just above threshold (features throughout) for 1D incoherent MI that leads to 1D filaments. Far above this threshold, at a much higher value of the nonlinearity, the 1D filaments become unstable (E) and become ordered in a regular 2D pattern (F).

below the threshold for 1D incoherent MI, at threshold, and just above the threshold. This shows (i) the existence of incoherent MI, and (ii) that incoherent MI occurs only when the nonlinear index change exceeds a well-defined threshold. In particular, Fig. 1C shows a mixed state exactly at threshold, in which order and disorder coexist. This is an indication that the nonlinear interaction undergoes an order-disorder phase transition, in agreement with the theoretical predictions (*8*). But the experiment, as often happens, revealed surprises. When the nonlinearity is further increased, a second threshold is reached: the filaments become unstable (Fig. 1E) and start to break into an ordered array of spots [two-dimensional (2D) filaments] as shown in Fig. 1F. In all the images in Fig. 1, the correlation distance is much shorter than the distance between two adjacent stripes or filaments. This is a clear demonstration that pattern can form in weakly correlated nonlinear multiparticle systems.

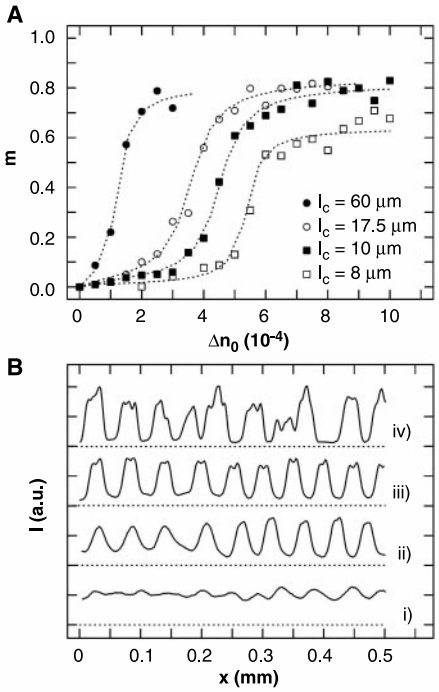

Fig. 2. Threshold dependence of incoherent MI. Modulation [$m = (I_{max} - I_{min})/(I_{max} + I_{min})$] of the light pattern versus size of the nonlinearity Δn_0 for different correlation distances l_c and an intensity ratio $I_0/I_{sat} = 1$. (**A**) Measured values of m for $l_c = 8$, 10, and 17.5 μm and for coherent light ($l_c \rightarrow \infty$). The dotted curves are guides for the eye. (**B**) Intensity cross sections of the stripes for $l_c = 17.5$ μm and a nonlinear refractive index change of $\Delta n_0 = 2.75 \times 10^{-4}$ (i), 4.0×10^{-4} (ii), 5.0×10^{-4} (iii), and 8.0×10^{-4} (iv). The dotted lines indicate the base line of the respective profile. The stripes emerge as sinusoidal stripes (for nonlinearity just above threshold), become square-wave stripes at a higher nonlinearity, and eventually break up into filaments at a large enough nonlinearity. a.u., arbitrary units.

Next, we studied the dependence of the MI threshold on the coherence properties of the beam. For a constant intensity ratio I_0/I_{sat}, the threshold where MI occurs depends on the incoherence of the light and on Δn_0 (which we control through the applied voltage V). To identify the MI threshold experimentally, one needs to examine the growth dynamics of perturbations and observe whether they grow or decay. This is difficult to measure, especially because the initial perturbations originate from random noise. Instead, we investigated the visibility (modulation depth) of the pattern observed at the output face of the crystal: random fluctuations that do not increase have a tiny (less than 5%) visibility, whereas the perturbations that grow emerge at high visibility (>50%) stripes. We have conducted numerous experiments with various degrees of coherence of the input beam, and measured the modulation depth of the output stripes as a function of the applied field (translated to Δn_0). The results are displayed in Fig. 2A, showing the modulation depth $m = (I_{max} - I_{min})/(I_{max} + I_{min})$ of the light at the output plane, as a function of Δn_0 for different correlation distances l_c and $I_0/I_{sat} = 1$. For a fully coherent input beam, m becomes large even at a vanishingly small nonlinearity because coherent MI has no threshold. When the correlation distance is reduced, however, a well-defined threshold is observed. The jump from very low visibility to a large visibility is always abrupt, because for every beam with a finite l_c there is always a threshold for MI. Clearly, the MI threshold shifts towards higher value of Δn_0 with decreasing correlation distance l_c.

Once the nonlinearity exceeds the MI threshold, the transverse frequencies that exhibit gain grow exponentially and form periodic patterns (Fig. 1). This growth leads to a large modulation depth (high visibility) in the output patterns and, equally important, to a considerable deviation of these stripes from a pure sinusoidal shape. That is, the propagation dynamics become highly nonlinear. Part of this dynamics was captured in the last figure in (*8*), by the appearance of the second spatial harmonic. Yet the experiment provides considerably more insight into the nonlinear dynamic evolution of the patterns, as displayed by the intensity cross sections of the stripes at the output plane in Fig. 2B. In this particular set of data, $l_c = 17.5$ μm and Δn_0 values 2.75×10^{-4} (i), 4.0×10^{-4} (ii), 5.0×10^{-4} (iii), and 8.0×10^{-4} (iv). At the lowest Δn_0 value, MI is barely above threshold (i). For the higher value at (ii), the modulation depth is higher yet the stripes have a sinusoidal shape. At the high value of (iii), the shape of the stripes is no longer sinusoidal, and several higher harmonics participate. For an even higher nonlinearity, the spectrum becomes irregular (iv), and 2D break up into filaments starts to occur.

The periodicity (or the spatial frequency) of the 1D filaments that emerge in the MI process depends on the coherence properties of the beam and on the magnitude of the nonlinearity (*8*). In all of our experiments, for any given intensity ratio, indeed the spatial frequency monotonically increases with increasing correlation distance and with increasing Δn_0.

Up to this point, the nonlinearity in our experiments had the form given in Eq. 1, which is not saturable. On the basis of the 1D incoherent MI theory (*8*), we expect that saturation of the optical nonlinearity should arrest the MI growth rate. To investigate saturation effects, we modified the nature of our photorefractive screening nonlinearity by launching a "flat top" beam that is narrower than the distance between the electrodes in our crystal, yet is wide enough to serve as a "quasi-uniform beam" at its flat top. Because the beam is finite, it does not contribute to the total current flowing through the crystal at steady state. Hence, the nonlinearity is now $\delta n = \Delta n_0 [I(r)/(I(r) + I_{sat})]$, which is the more commonly used form of the photorefractive screening nonlinearity (*20*, *21*), and it has a saturable nature. When we launch such

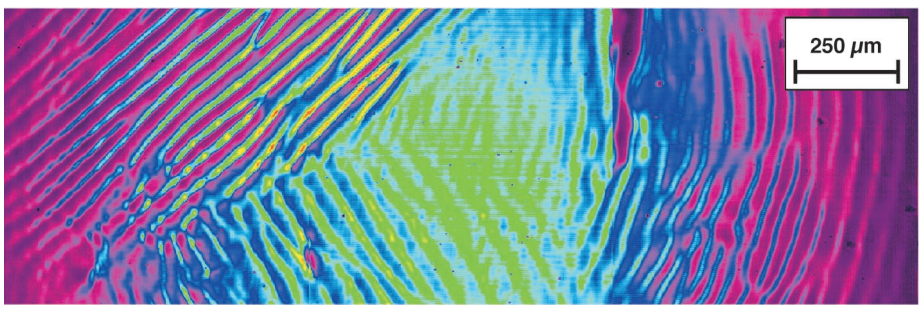

Fig. 3. Suppression of incoherent MI due to saturation of the nonlinearity. The intensity structure of a finite signal beam [Gaussian beam with a width (FWHM) of 1 mm] at the output plane of the crystal. The intensity ratio (peak of beam to background/saturation intensity) is $I_0/I_{sat} = 3$. Without nonlinearity ($\Delta n_0 = 0$), the output beam shows no features. The photograph is taken at $\Delta n_0 = 6 \times 10^{-4}$. The saturable nature of the nonlinearity clearly suppresses MI in the center of the beam, whereas strong modulation and filaments of random orientation occur in the margins of the beam.

a beam in a biased crystal with $\Delta n_0 = 6 \times 10^{-4}$ and with a ratio between the peak intensity and the saturation intensity, $I(0)/I_{sat} = 3$, patterns form in several regions on the beam (Fig. 3). At the flat top of the beam, low visibility stripes appear. In this region, the nonlinearity is above threshold but in rather deep saturation, so the MI growth rate is suppressed. Then, at the margins of the beam, where the local ratio $I(r) + I_{sat}$ is around and slightly below unity, high-visibility stripes appear. In this region, the nonlinearity is above threshold and is not saturated, so the MI growth rate is large. Lastly, at the far margins of the beam, the local nonlinearity is below threshold, because $I(r) \ll I_{sat}$. A by-product of this particular experiment is the clear evidence (Fig. 3) that the 1D stripes emerge at different orientations and are not affected much by the local noise (striations).

We would also like to relate our nonlinear optical system to other nonlinear systems of weakly correlated particles. Our prediction and experimental observation implies that in such systems patterns will form spontaneously, provided the nonlinearity is larger than a threshold value, which in turn is set by the correlation distance. For example, we expect that 1D and 2D patterns will form in an atomic gas at temperatures slightly above the Bose-Einstein condensation temperature (at which the atoms possess independent degrees of freedom, yet are still weakly correlated). At least for atoms with attractive collision forces, whether natural [e.g., ^{7}Li (*23*)] or through magnetic tuning of the condensate self-interaction (*24*), such patterns should form. The equation governing the evolution of the "mean field" of an atomic gas is the Gross-Pitaevski equation (*25*), which almost fully coincides with the nonlinear wave equation that gives rise to (1+1)D Kerr solitons. The relevance of this work to cooled atomic gases is therefore obvious. In other areas of physics there are, in fact, at least some hints that such patterns do exist in disordered many-body nonlinear systems. To be specific, several experimental papers have reported a large anisotropy in the resistivity of a 2D electron system with weak disorder (*26*). The observed anisotropy is now attributed to the combination of nonlinear transport and weak disorder (*27*, *28*), which is the transport equivalent of nonlinearity and incoherence in optical systems such as ours. The theoretical works predict the existence of 1D stripes (electron stripes) of charge density wave. Spontaneous formation of stripes was also predicted and observed in high-T_c (superconducting transition temperature) superconductors (*29*), which is again a nonlinear weakly correlated many-body system. Lastly, as discussed in (*8*), spontaneously forming patterns are known in at least one system of classical particles: a gravitational system. The spontaneous emergence of patterns in all of these diverse fields of science indicates that pattern formation in nonlinear weakly correlated systems is a universal property. It is a gift of nature that in optics we can study directly, visualizing every little detail of the physics involved and isolating the underlying effects.

References and Notes

1. V. I. Bespalov and V. I. Talanov, *JETP Lett.* **3**, 307 (1966).
2. V. I. Karpman, *JETP Lett.* **6**, 277 (1967).
3. A. Hasegawa and W. F. Brinkman, *J. Quant. Electron.* **16**, 694 (1980).
4. For a review on MI in the temporal domain, see G. P. Agrawal, *Nonlinear Fiber Optics* (Academic Press, San Diego, CA, ed. 2, 1995), chap. 5 and references therein.
5. M. D. Iturbe-Castillo *et al.*, *Opt. Lett.* **20**, 1853 (1995).
6. M. I. Carvalho, S. R. Singh, D. N. Christodoulides, *Opt. Commun.* **126**, 167 (1996).
7. For a recent review on optical spatial solitons, see G. I. Stegeman and M. Segev, *Science* **286**, 1518 (1999).
8. M. Soljacic, M. Segev, T. H. Coskun, D. N. Christodoulides, A. Vishwanath, *Phys. Rev. Lett.* **84**, 467 (2000).
9. T. H. Coskun, D. N. Christodoulides, Y. Kim, Z. Chen, M. Soljacic, M. Segev, *Phys. Rev. Lett.* **84**, 2374 (2000).
10. M. Mitchell, Z. Chen, M. Shih, M. Segev, *Phys. Rev. Lett.* **77**, 490 (1996).
11. M. Mitchell and M. Segev, *Nature* **387**, 880 (1997).
12. D. N. Christodoulides T. H. Coskun, M. Mitchell, M. Segev, *Phys. Rev. Lett.* **78**, 646 (1997).
13. M. Mitchell, M. Segev, T. H. Coskun, D. N. Christodoulides, *Phys. Rev. Lett.* **79**, 4990 (1997).
14. A. W. Snyder and D. J. Mitchell, *Phys. Rev. Lett.* **80**, 1422 (1998).
15. V. V. Shkunov and D. Z. Anderson, *Phys. Rev. Lett.* **81**, 2683 (1998).
16. Z. Chen, M. Mitchell, M. Segev, T. H. Coskun, D. N. Christodoulides, *Science* **280**, 889 (1998).
17. D. N. Christodoulides, T. H. Coskun, M. Mitchell, Z. Chen, M. Segev, *Phys. Rev. Lett.* **80**, 5113 (1998).
18. N. Akhmediev, W. Krolikowski, A. W. Snyder, *Phys. Rev. Lett.* **81**, 4632 (1998).
19. O. Bang, D. Edmundson, W. Krolikowski, *Phys. Rev. Lett.* **83**, 4740 (1999).
20. M. Segev, G. C. Valley, B. Crosignani, P. DiPorto, A. Yariv, *Phys. Rev. Lett.* **73**, 3211 (1994).
21. D. N. Christodoulides and M. I. Carvalho, *J. Opt. Soc. Am. B* **12**, 1628, (1995).
22. M. Shih, M. Segev, G. C. Valley, G. Salamo, B. Crosignani, P. DiPorto, *Electron. Lett.* **31**, 826 (1995).
23. C. A. Sackett, J. M. Gerton, M. Welling, R. G. Hulet, *Phys. Rev. Lett.* **82**, 876 (1999).
24. S. L. Cornish, N. R. Claussen, J. L. Roberts, E. A. Cornell, C. E. Wieman, *Phys. Rev. Lett.* **85**, 1795 (2000).
25. Th. Busch and J. R. Anglin, *Phys. Rev. Lett.* **84**, 2298 (2000).
26. M. P. Lilly, K. B. Cooper, J. P. Eisenstein, L. N. Pfeiffer, K. W. West, *Phys. Rev. Lett.* **82**, 394 (1999); *Phys. Rev. Lett.* **83**, 824 (1999).
27. A. A. Koulakov, M. M. Fogler, B. I. Shklovskii, *Phys. Rev. Lett.* **76**, 499 (1996).
28. A. H. MacDonald and M. P. A. Fisher, *Phys. Rev. B* **61**, 5724 (2000).
29. V. J. Emery *et al.*, *Proc. Natl. Acad. Sci. U.S.A.* **96**, 8814 (1999), and references therein.

30. Supported by the Israeli Science Foundation, the National Science Foundation, the Army Research Office, the Air Force Office of Scientific Research, and the Deutsche Forschungsgemeinschaft. This work is part of the Multi University Research Initiative (MURI) project on optical spatial solitons.

2 June 2000; accepted 31 August 2000

Experimental Verification of Decoherence-Free Subspaces

Paul G. Kwiat,[1]* Andrew J. Berglund,[1]† Joseph B. Altepeter,[1] Andrew G. White[1,2]

Using spontaneous parametric down-conversion, we produce polarization-entangled states of two photons and characterize them using two-photon tomography to measure the density matrix. A controllable decoherence is imposed on the states by passing the photons through thick, adjustable birefringent elements. When the system is subject to collective decoherence, one particular entangled state is seen to be decoherence-free, as predicted by theory. Such decoherence-free systems may have an important role for the future of quantum computation and information processing.

Quantum computation holds the promise of greatly enhanced speeds for solving certain problems, including factoring (*1*), simulation of quantum systems (*2, 3*), and database searching (*4, 5*). One main obstacle to quantum computation is the problem of decoherence—fragile quantum superpositions are destroyed by unwanted coupling to the environment. In particular, it is the entangling of the quantum system to unobserved degrees of freedom that leads to a loss of coherence. (A related problem is that of dissipation, whereby energy is lost from the system.) Three basic strategies to cope with decoherence in quantum computation have emerged. The first, quantum error correcting codes, relies on trying to detect errors using ancillary quantum bits (qubits) and actively manipulating the interactions to correct these errors (*6, 7*). The second strategy employs dynamical decoupling, in which rapid switching is used to average out the effects of a relatively slowly decohering environment (*8*). The final approach attempts to embed the logical qubits

[1]Physics Division, P-23, Los Alamos National Laboratory, Los Alamos, NM 87545, USA. [2]Physics Department, University of Queensland, Brisbane, Queensland 4072, Australia.

*To whom correspondence should be addressed. E-mail: kwiat@lanl.gov

†Present address: Physics Department, California Institute of Technology, Pasadena, CA 91125, USA.